Estimation of the neutrino rest mass from measurements of the tritium β spectrum

V. A. Lyubimov, E. G. Novikov, V. Z. Nozik, E. F. Tret'yakov, V. S. Kozik, and N. F. Myasoedov

Institute of Theoretical and Experimental Physics
(Submitted 22 May 1981)
Zh. Eksp. Teor. Fiz. **81**, 1158–1181 (October 1981)

Measurements of the tritium β spectrum near the end point and the analysis of the results are described. In comparison with our earlier study [E. F. Tret'yakov *et al.*, Bull. Acad. Sci. USSR, Phys. Ser. **40**, No. 10, p. 1 (1976) and as reported at the Aachen 1976 Neutrino Conference (p. 663)], the statistical accuracy has been greatly improved and a more rigorous measurement technique has been used. All data obtained in the two studies have been analyzed. In determining the confidence interval for the antineutrino rest mass, the method of mathematical modeling is used. For the rest mass of $\tilde{\nu}_e$ a lower limit is obtained for the first time: $14 \leq M_{\tilde{\nu}_e} \leq 46$ eV. The value $E_0 = 18\,577 \pm 13$ eV is obtained for the energy of tritium β decay.

PACS numbers: 14.60.Gh, 23.40.Bw, 27.10. + h

I. INTRODUCTION

The present work is a continuation of measurements of the tritium β spectrum begun in 1975 for the purpose of improving the data on the antineutrino rest mass.[1] A brief report of the results of the present work has been published in a letter.[2] The results have been obtained on the basis of analysis of the entire set of experimental data, including that of Ref. 1.

In our letter[2] we indicated the probable existence of a finite rest mass of the antineutrino. In view of the importance of this assertion, in the present article we discuss in detail the most important aspects of the experiment and of the analysis of the results. The changes in the experimental apparatus which were made in comparison with Ref. 1 are described.

The method of determination of the antineutrino rest mass from the shape of the tritium β spectrum has been used repeatedly, beginning at the end of the 1940's.[3-12] It is based on the fact that the phase space of the β-decay electrons

$$A(z) \to A(z+1) + e^- + \tilde{\nu}_e \qquad (1)$$

changes as a result of the energy expended in creation of the antineutrino rest mass. The nature of the change can be seen from the formula for the phase space, which describes the basic energy dependence of the β spectrum:

$$dS(p) \sim p^2 (E_0 - E)\,[(E_0 - E)^2 - M_\nu^2]^{1/2} dp. \qquad (2)$$

Here E_0 is the decay energy, M_ν is the rest mass of $\tilde{\nu}_e$, and p and E are the momentum and kinetic energy of the β particle.

For all the smallness of M_ν ($M_\nu \ll E_0$) this kinematic effect is the basis of the most sensitive direct method of measurement of the rest mass of $\tilde{\nu}_e$. Tritium is used not only as a result of the smallness of the end-point energy ($E_0 \approx 18.6$ keV), but also as a result of the high rate of the superallowed transition. Of course, the simplicity of the nuclei taking part in the reaction also has a special importance.

II. EXPERIMENTAL APPARATUS

The energy analysis of the β spectrum of tritium was carried out, as before,[1] in the iron-free toroidal β spectrometer of our institute with fourfold deflection of the electrons.[13] Nonequipotential sources were used according to the method of Bergkvist.[11,1] Among the advantages of the β spectrometer of Ref. 13 are the extremely low background of scattered electrons. In sensitivity (luminosity) it is inferior by an order of magnitude to Bergkvist's apparatus, which he used for measurement of the β spectrum for the same purpose. In Ref. 1 the lack of sensitivity was compensated as the result of use of stronger sources of tritiated valine and increase of the measurement time. The statistics collected in the present work is three times that obtained in Ref. 1. The resolution of the spectrometer with the nonequipotential source was unchanged in comparison with Ref. 1 and amounted to 0.12% in momentum (focusing current). As previously, the tritiated material was valine ($C_5H_{11}NO_2$) with 18% enrichment in tritium (about two atoms per molecule). The material for the calibration measurements was Yb^{169}.

1. Proportional detector

In the 1975 experiments published previously,[1] the detector was a low-pressure Geiger counter. A strong feature of such a detector was the high efficiency for detection of β electrons and, as a result, a practically complete lack of dependence of the efficiency on energy. However, an unpleasant aspect was the fact that tritium which evaporated from the source during the run contaminated the spectrometer volume and raised the general background level. While the background in the clean spectrometer was at the level ~0.05 counts per second, which practically corresponds to the external background, by the end of the 1975 measurements it had increased almost an order of magnitude, thus making further collection of statistics inefficient.

Since a Geiger counter responds to the passage of particles without distinguishing them on the basis of

 0038-5646/81/100616-13$02.40

energy, the contribution to the background from the tritium distributed over the spectrometer volume gave the entire spectrum, the maximum of which lies in the region ~6 keV. The natural means of fighting the background was to use as detector a proportional counter. This mode requires increasing the pressure in the counter, in order that the range of the tritium β electrons fall in the sensitive volume of the counter. For this purpose the collodion film of the entrance slit was replaced by lavsan polyester with thickness 150–200 $\mu g/cm^2$. Its mechanical strength is such that when supported by wires stretched across the slit every 1 mm it will maintain a pressure up to two bars. The working gas is argon with addition of methyl or ethyl alcohol. The resolution of the counter in energy was 6 keV. The main part of the background from tritium was cut off by introduction of pulse-height discrimination of the counter pulses. This possibility is easily evident from comparison of the pulse-height spectra for the electrons of the β spectrum and the background in Fig. 1. Usually the threshold was set so that the counter efficiency was ~50%. Here the background was reduced to a value ~0.05 counts per second.

In the present work the background level was assumed constant in the energy range studied. This is confirmed by measurements without a source (see below) and by the agreement of the background levels in the region $E > E_0$ measured with the working source and without it.

The next change in the detector was made for the purpose of increasing the rate of collection of information. Instead of a single counter we used a three-channel proportional chamber. The three sensitive volumes were located in a single block of copper with a distance of 7.5 mm between the wires. The length of the chamber was 40 mm. On the spectrometer-coil side the chamber was covered with flanges with three windows. The sensitive volumes of the chamber were separated by metal and did not affect each other. Thus, during a run with a given spectrometer current, the β spectrum was measured simultaneously at three points in energy, shifted in accordance with the dispersion of the apparatus by approximately 75 eV. The channel closest to the source was given the designation +1, the center channel 0, and the furthest channel −1.

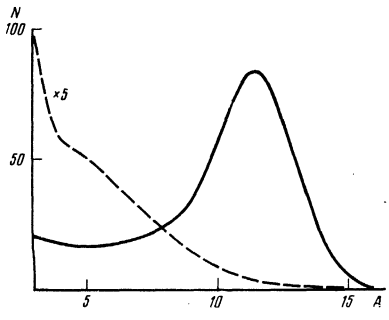

FIG. 1. Pulse-height spectra of the signal from the proportional detector. Measurement with the working source with settings, E=18 489 eV (solid curve) and E = 18 700 eV (dashed curve).

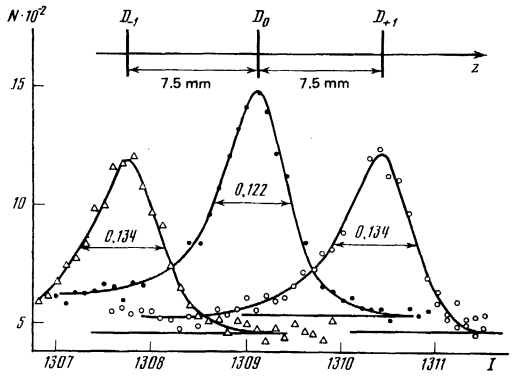

FIG. 2. The M_{III} line (E = 18 849 keV) measured simultaneously in the three channels of the three-channel chamber. The abscissa scale is the focusing current. The numbers give $\Delta I/I$ in %. The distance between the peaks is 73 eV. In the upper part of the figure we have shown the location of the sensitive wires of the three-channel chamber.

Figure 2 shows a diagram of the three-channel chamber and the spectrum of the M line[1)] for all channels of this detector. As a result of imperfection in the focal plane in the toroidal spectrometer the instrumental line shapes (resolution functions) are different in each of the channels, and in the subsequent analysis of the results they were established individually for each channel. The calibration was also carried out individually. Thus, the three β spectra measured in one run are independent experiments.

Use of the three-channel detector increased the rate of collection of information by 2.5 times, so that at the end of this work, with 50% efficiency of the detector, it was higher than in Ref. 1 and with a lower background.

2. Changes in the electron source

In Ref. 1 we noted a discrepancy with Bergkvist[11] in the value of the β-decay energy. In order to increase the accuracy of measurement of the energy, in the later experiments we improved the source of electrons. In a single frame, i.e., at a fixed distance apart two nonequipotential sources of electrons were mounted: the main source of tritium β particles at the bottom, close to the detector, and the calibration source at the top. The frame had a gap in the middle between the sources. It could be placed with either its base or the edge of its gap fastened to a tilted slide. In the former case the main source was at the focus, and in the latter the calibration source could be exposed. The source was changed without breaking the vacuum by raising or lowering the frame. By exposing the calibration source it was possible at any time to check the normal operation of the spectrometer, the standard resistor,[2)] and the Weston standard cell. The two sources were connected in parallel to a voltage divider to provide the focusing potentials. From the shape of M_I line it was possible to monitor this system also. (Inaccuracy in the source of focusing potentials cannot be observed on the basis of the continuous spectrum.) The double source was introduced in the runs with the three-chan-

nel detector.

During the measurement of the β spectrum, the calibration source was located in a lead pocket. The adequacy of the shielding was evaluated in experiments in which the main source was replaced by clean aluminum sheets. The background in the region of the tritium β spectrum was measured. The results are shown in Fig. 3. From this experiment it was concluded that the distortion of the spectrum is insignificant.

In the intervals between runs with the working source we measured (about once a day) the position of the peak of the M_I line (18.4 keV) of the calibration source. As it worked out, we used for the calibration a lavered source—Yb covered by a 50% (relative to the thickness of the working source) layer of the tritiated material.[3)] (Here we had the possibility of evaluating the stability of the tritiated layer with time on the basis of the line shape.) In Fig. 4 we have shown the results of four-week measurements with the three-channel chamber. The possible insignificant shift of the average value of the peak position with time can be explained by a decrease of the source thickness. The rms deviation for the worst case (channel +1) is $2 \cdot 10^{-3}$% in current, which corresponds to an energy uncertainty less than 1 eV. If we assign this value to instability of the installation of the calibration source in its operating location (1 eV corresponds to 0.1 mm along the spectrometer axis), we can hope that the main source is positioned with the same or better accuracy. This hope is supported by the additional argument that the main source is mounted on the support by its base.

In the experiments with the three-channel detector we also took measures to permit almost continuous following of the stability of the standard source of emf. For this purpose approximately every three hours we measured the emf of the three standard cells. Their stability is guaranteed with high reliability by the constancy of a primary cell.

3. Measurement procedure

As in Ref. 1, in scanning the spectra we used a device which automatically changed the focusing current in steps. Switching was accomplished after a 100-second measurement period for the working source or a 30-second period for the calibration source. The measurement time was set by a quartz generator. We shall call the current at which the spectrum was measured for a specified time a channel. The distance between channels is ≈8.5 eV. The automatic control first

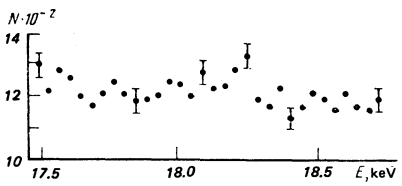

FIG. 3. Background spectrum. At the main source location we have placed the aluminum substrates. The calibration source is in a lead shield. Measurement time $1.7 \cdot 10^4$ sec/channel.

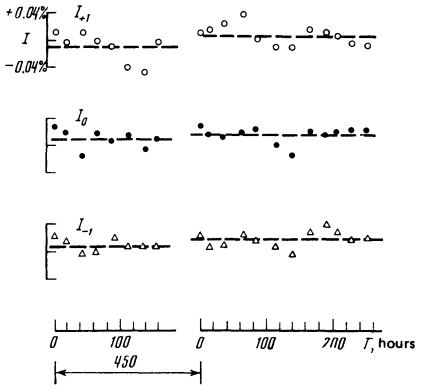

FIG. 4. Coordinates of the maximum of the calibration peak measured between β-spectra runs with the three-position detector. The ordinate is the focusing current at the maximum of the peak. (The width of a current channel in the calibration peak measurements in relative units is $2.3 \cdot 10^{-4}$.)

increased the current, and then decreased it to its initial value. The complete excursion of the automatic control gives a measurement time in each channel of 200 seconds (or 60 seconds). The control permitted measurement of the spectrum in a maximum of 56 channels. At equal current intervals, this covers about 450 eV. In measurement of larger regions of the spectrum it was necessary to set several initial values of the current. The distance between these initial currents was ordinarily chosen equal to 50 channels, with six channels overlapping. The current stabilization and switching circuits were such that the distance between channels was not constant and depended on the number of the interval. With the chosen interval ≈8.5 eV, the greatest deviation of the current from the nominal value determined on the basis of the channel number at equal intervals was −0.5 eV for channel 40 and +0.5 eV for channel 50.

From the point of view of the accuracy of the sought physical quantities, it is advantageous to have a measurement plan in which the length of run is increased towards the end point of the β spectrum with increasing energy. In the experiments with several initial currents it was possible to accomplish this plan, assigning a larger number of steps of the automatic control at the end of the spectrum ($E \approx E_0$). A measurement cycle with two initial currents was carried out in the following sequence: one step with a small initial current, then two with a larger initial current, and so forth. In this way the repeated measurements of the spectrum in the same channel at different times should have cancelled the drift of the entire apparatus, giving the systematic deviations a statistical nature.

A digital printer was used to record the information. For auxiliary purposes, recording with mechanical counters was retained. In the experiments with the three-channel detector the mechanical counters recorded the pulses from the channel with index zero with a low discrimination level.

4. Energy calibration of the β spectrometer

The energy calibration procedure was the Siegbahn

autocalibration method[14] which we used in Ref. 1. This made use of the electron internal conversion lines L_I, L_{II}, L_{III}, M_I, M_{II}, M_{III}, and N_I of the 20.74-keV γ transition. On the basis of these data the constants E_γ and η were found for the equation relating the energy and the momentum of electrons focused by the iron-free magnetic β spectrometer:

$$E_i=[(1+\eta I_i^2)^{1/2}-1]M_e=E_\gamma-E_{b\text{-}i}, \quad (3)$$

where i is the designation of the subshell, I_i is the focusing current[4] for internal conversion electrons from this subshell, and E_{b-i} is the binding energy for this subshell (taken from Ref. 15). Equation (3) has been written down on the assumption that for the magnetic spectrometer the relative resolution in momentum $\Delta p/p = \text{const}$.

As a supplement to the calibration measurements of 1975 we carried out calibrations with a single proportional counter and independent calibrations for all three channels with the three-channel chamber.[5)]

An attempt was made to estimate the influence of the electric field of the coil on the electron energy. In Eq. (3) we introduced a term which contains the coil potential as an unknown parameter. The best agreement is achieved for a value of the potential close to zero. The average potential of the wires of the coil with respect to the source for the current corresponding to 18.6 keV is +7 volts. In a special experiment in which the average potential of the wires was increased by 8.5 volts, the shift of the location of the M_I line was 1.6 eV.

For the parameter E_γ we obtained the value 20 735 ± 2 eV in measurements with proportional counters and correspondingly $\Delta\eta/\eta = 5 \cdot 10^{-5}$.

A calibration was always carried out before the working measurements.

5. Instrumental line shape

The instrumental line shape or resolution function R is an important characteristic of measuring apparatus. The reliability of the determination of this function takes on special significance when the effect under investigation, the influence of the neutrino rest mass on the shape of the β spectrum, is comparable with or less than the distortions produced by the apparatus. In this case the effect can be made visible only by means of a statistical analysis.

In the present work the resolution function was determined by the layered-source method described in Ref. 1. In view of the special importance of this characteristic of the apparatus, the procedure for determining the resolution function is set forth here in more detail.

The essence of the method is to pass monoenergetic electrons through a layer of source material containing the tritium. From the intensity of the β spectrum it is possible to judge the relative thickness of the layer on the substrates, and from the change in the line shape of the monoenergetic electrons it is possible to judge the optical properties of the spectrometer and the stopping power of the layer.[6)] By obtaining measurements of spectra with several layered sources of different thickness, it is possible to establish the instrumental line shape for a source of tritium electrons with the working thickness (intensity). The procedure for establishing the line shape is based on the natural assumption that the working source can be represented as consisting of a finite number of electron-emitting thin layers separated by layers of inactive stopping material.

Measurements were made with standard nonequipotential sources (see Ref. 1) of 18 substrates made up of nine pairs with the clean sides facing each other. To obtain the function with the zeroth layer of tritiated material we used the M_I, M_{II}, and M_{III} lines measured with the ytterbium source. These lines have energies 18.42, 18.65, and 18.85 keV, which very conveniently encompasses the end point of the tritium β spectrum. For our purposes the ytterbium sources can be considered infinitely thin. This statement is illustrated by Fig. 5, where we have combined the M_I lines measured with sources whose intensities differed by a factor of two. The sources were made from the same solution and were exposed almost simultaneously. The almost complete coincidence of the lines is evident from the figure.

The ytterbium source was prepared under the same conditions as the main source, in six evaporations. We then measured the portion of the spectrum containing the M lines. It is shown in Fig. 6.[7)] After this the substrates were again placed in the evaporation chamber and a layer of tritiated material deposited on them. For this purpose we deposited a water-alcohol solution of valine on a tungsten ribbon, but unfortunately the spectrum of the chemical materials on the substrate after the evaporation is unknown to us. We took measures to assure that the calibration (layered) sources and the main sources (for measurement of the β spectrum) would have identical composition of the material containing the tritium, including, of course, the impurities.

The instrumental lines were determined independently for the experiments with the single counter and for each channel of the three-channel proportional cham-

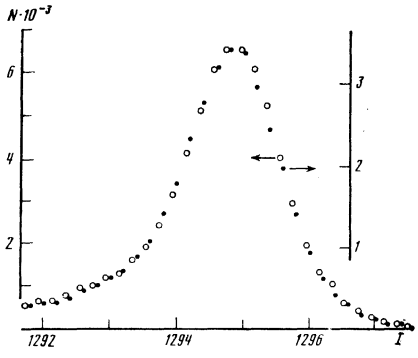

FIG. 5. The shape of the M_I line ($E = 18.42$ keV) from a Yb source with intensities differing by a factor of two. The two sources were prepared in the same day and are located on a single frame.

ber. In the 1976 experiments the determination of the line shape and the data run were made with valine from different lots. Here the stopping powers of the material in the lots were compared and turned out to be identical. In the 1978 experiments the calibration layered sources were made and measured before preparation of the main source from the same solution.

In constructing the instrumental line shape of pure ytterbium, we took as a basis the M_{II} line, since the M_I line, which has six times higher intensity, is broadened[8] by ~8%. The region of determination of the instrumental line is equal to 86 channels: 15 at higher electron energies (+) and 70 at lower electron energies (−). The zero channel coincided with the tip of the peak, and the intensity in it was taken as unity. The interval between the channels was the same as in recording the β spectrum. From Fig. 6 it is evident that the lines are not completely separated, and therefore on the basis of the M_{II} line we can construct only part of the zero instrumental line both in the positive channels and the negative channels. To determine the wing on the high-energy side we used the right-hand edge of the M_{III} line exposed for a longer time. In the negative channels (from −12) the spectrum was constructed from the shape of the M_I line, with correction for the broadening up to channel −30. For the more remote channels the spectrum of the M_I line was not corrected. As background we took the minimum intensity of the spectrum between the M_{III} and N_I lines. The maximum for the instrumental line of pure ytterbium is the point for which the energy calibrations were made. The width of this line at half-height was 45 eV.

Construction of the instrumental lines for layered sources with different thickness of tritiated material was carried out by the same means. The increase of the width as a result of the energy loss resulted in poorer separation of the lines. The accuracy in determination of the intensity in the negative channels was greatly decreased as a result of the need for subtraction of the spectrum of tritium electrons from the combined spectrum.

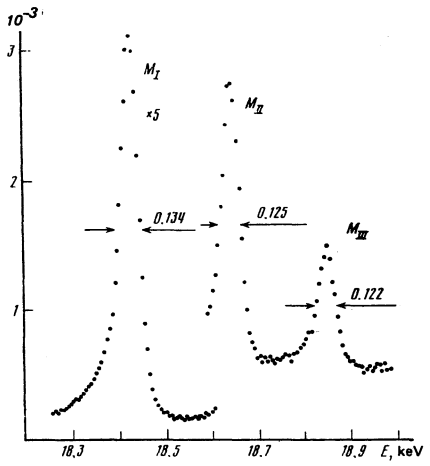

FIG. 6. Spectrum of the M lines of the transition $E_\gamma = 20.74$ keV. The source is pure ytterbium. The measurement time is 60 sec. Measured with channel 0 of the three-channel chamber. The numbers indicate the relative value of $\Delta p/p$ in %.

In the experiments with a single counter we used layered sources with thicknesses 0.2, 0.45, and 0.67 of the thickness of the layer of the main source, and in the experiments with the three-channel chamber we used layered sources with thickness 0.5, 0.9, and 1.3.[9] The shift of the peak of the line obtained in these experiments as a function of the thickness of the layer turned out to be linear: ~0.8 eV for 10% of the layer thickness.

The next step was to construct instrumental lines for five layers of tritiated material equidistant in thickness (0, 0.2, 0.4, 0.6, and 0.8). The intensity in the channels for these lines was found by interpolation or extrapolation of the values for the measured layers. After smoothing and normalization, all five functions were added—this is the instrumental line shape or resolution function of the spectrometer for the main source, R, which will be used in analysis of the tritium β spectrum.

For illustration of the method we have shown in Fig. 7 M_I lines measured with layered sources of thickness 0, 0.5, and 0.9 (respectively the dots, circles, and triangles). Here the solid curve shows the resolution function for the main source of tritium.

As a very important circumstance we note the coincidence of the main function and the function for the ytterbium source with valine of half thickness. Such should be the case according to the calculations of Soloshchenko,[16] if the stopping layer is sufficiently thin and the quadratic corrections to the linear dependence of the monoline transmission spectrum on the thickness are small. We consider this agreement as an indirect confirmation of the correctness of construction of the resolution function for the main source. Soloshchenko[17] calculated monoline transmission spectra for various thicknesses of the stopping layer. Good agreement with the experimental transmission function was obtained for a valine layer thickness 2 $\mu g/cm^2$.

The error in our determination of the intensity in the channels of the function R is estimated as 10% at the half-width and 50% in the wings.

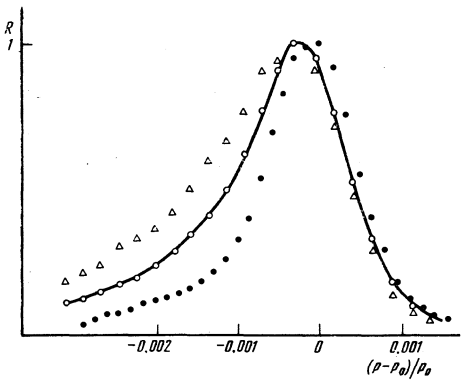

FIG. 7. The instrumental line for layered sources. The thickness of valine of the working source was taken as 1: ●—pure Yb, ○—Yb+ 0.5 valine, △—Yb+ 0.9 valine; the solid curve shows the complete instrumental line for the working source.

6. Energy dependence of detector efficiency

It is obvious from general considerations that the change with energy of the efficiency for detection of the electrons focused by the β spectrometer will produce a distortion of the tritium β spectrum. By using for analysis of the experimental data a method which determines the shape of the β spectrum without taking into account this effect, it is possible to erroneously accept these distortions as the result of a manifestation of a finite rest mass of the antineutrino. The detector efficiency must be either measured, or determined on the basis of the measured β spectrum by introducing into the shape of the spectrum some parametric dependence. The contribution of the correction function for the working energy range must be sufficiently small so that the error in its determination does not lead to an appreciable effect in the mass.

As will be mentioned below, in determination of the physical quantities we did not use independent measurements of the efficiency, but employed a parametric description of the measured β spectrum. Nevertheless it is worth mentioning that an experimental estimate of the magnitude of this effect was made in the experiments with the three-channel chamber. In analysis of the counting rate of tritium electrons in the measurements with a discriminator and of the pulse-height spectrum of the signals at several points in energy, it turned out that the energy dependence can be represented by a linear function $1+\alpha(E-18\,580)$ with $\alpha=1.4\times10^{-4}$ eV^{-1}. For a 700-eV range the contribution of the linear term is ~10%. The results are identical for all three channels. The crude approximations made in this analysis permit us to use this estimate only for the scale of the effect.

In the same series of calculations we made an estimate of the energy dependence of the reflection and transmission of the films covering the entrance slit of the detector. For this purpose we measured the intensity of a number of electron internal conversion lines with films of four thicknesses: 0.15 mg/cm^2 (the working film), 0.3, 1.4, and 3.6 mg/cm^2. The ratio of the intensities was interpreted as the change in the electron transmission with energy. We estimate the maximum effect as 3% in 700 eV at an average energy 18.4 keV.

We emphasize again that these estimates were not actually used in analysis of the β spectra.

III. ANALYSIS OF THE EXPERIMENTAL DATA

All of the experimental data subjected to analysis are contained in 16 runs. We define a run as a set of data on the β spectrum obtained in a continuous cycle of measurements. It is assumed that within a run there are no changes in the entire apparatus. The interval between runs consists of several days up to several years. The runs may differ in the length of the measured portion of the β spectrum, the duration of the measurement, the background, or changes in the apparatus. The runs cannot be mechanically combined.

Some data are given in the table. The runs are numbered in chronological order. Runs 1–4 were carried out with a Geiger counter. Runs II and III, reported in Ref. 1, are combined here into run 1, and run V corresponds here to run 4. Runs 5–8 were made with a proportional counter. Run 8 was taken with a high discrimination threshold. Runs 9–16 were taken with the three-channel chamber: channel 0—runs 9, 10, 11, and 14; channel +1—runs 12 and 15; channel −1—runs 13 and 16. Runs 9 and 10 were taken with a low discrimination threshold simultaneously with runs 11 and 14. In the fourth line of the table we have given the measurement duration in the measuring channel for the region $E\sim E_0$. In the fifth line of the table we have given the intensity of the spectrum after subtraction of background in the channel corresponding to energy 18 475 eV.

The extraction of the physical quantities contained in the measured β spectrum is considered in the first stage of the analysis to be a problem of mathematical statistics. Obviously such a solution cannot be considered unique. As will be clear below, the instrumental distortions of the spectrum and the deformation of the three-particle phase space of the electrons as the result of atomic and molecular processes are similar in shape and magnitude (but opposite in sign) to the effect of a massive neutrino. Therefore in determining the limits of the confidence interval in the second stage of the analysis we shall test those hypotheses which correspond to the minimum possible neutrino mass.

1. Model of the β spectrum

Let us show how one can represent the number of electrons recorded by the spectrometer for a fixed focusing current. The corrections introduced into the spectrum will be evident.

Let $Q(p')$ be the number of electrons actually emitted by the source in the momentum interval p', $p'+\Delta p'$. For a current I the spectrometer will record electrons in a momentum interval $p, p+\Delta p$. If $R(p',p)$ is the probability that an electron emitted by the source with momentum p' will be recorded by the detector as an electron with momentum p, then for the number N of electrons measured in channel I we can write the expression

$$N(p(I))=\Delta p(I)\int Q(p')\varphi(p')R(p',p)\,dp'. \tag{4}$$

Here $p(I)$ is the known relation between the spectrometer current and the electron momentum, obtained in the calibration measurements, and φ is the detection efficiency. The function $R(p',p)$ is the instrumental line shape discussed above.[10] If we had a source of monoenergetic electrons with constant intensity for all energies, we would obtain experimentally complete information on $R(p',p)$. In reality a complete reconstruction is carried out for a single value of p. Therefore in what follows we shall assume that the resolution function is the same for all p, and its small variations in the energy range investigated we shall take into account in the form

$$R(p',\,p)=R(p-p')\varepsilon(p'),$$

TABLE I.

Number of run	1	2	3	4	5	6	7	8	9	10	11	12	13	14	15	16
Date	1975				1976				1978							
Number of points	55	110	110	55	168	168	30	44	112	112	112	112	112	112	112	112
Duration, seconds per channel	5600	2800	3600	8700	5600	6600	12400	40000	6000	9200	6000	6000	6000	9200	9200	9200
Effect, sec^{-1} $channel^{-1}$	0.17	0.13	0.14	0.14	0.11	0.08	0.08	0.06	0.16	0.10	0.12	0.10	0.11	0.09	0.11	0.07
Background, sec^{-1} $channel^{-1}$	0.11	0.15	0.18	0.30	0.06	0.06	0.05	0.01	0.35	0.46	0.07	0.07	0.05	0.10	0.11	0.07
χ_N^2	1.17	1.12	1.02	1.02	1.05	1.12	1.12	1.2	0.99	1.21	1.2	1.21	1.23	1.37	1.22	1.09
		1.12				1.18				1.11				1.25		
M_ν, eV	22.8	9.1	37.5	0	49.0	31.1	48.5	21.6	35.4	40.5	42.0	31.4	44.4	25.8	57.7	42.4
		11.7				39.3				38.4				37.4		
E_0, eV	78.5	73.0	79.5	81.0	78.9	65.8	77.1	63.6	76.4	79.5	80.0	75.0	84.4	76.9	85.2	84.4
18500+		76.0				71.7				78.2				79.0		
$\alpha \cdot 10^4$, eV^{-1}	−0.28*	0.07	−0.5	−0.28*	1.1	1.5	1.2*	1.2*	1.4	1.12	1.45	1.28	0.65	1.8	0.84	0.65
		−0.29				1.37				1.22				–		
$\alpha\Delta E \cdot 10^2$	−1.9*	0.5	−3.5	−1.9*	7.7	10.5	8.4*	8.4*	9.8	7.8	10.5	9.0	4.5	12.6	6.0	4.5
		−2.0				9.6				8.5				–		

Note. The symbol * denotes a fixed value of the parameter.

where ε takes into account the dependence of the shape of the resolution function on the energy. Equation (4) then takes the form

$$N(I)=Ap\int Q(p')\varphi(p')\varepsilon(p')R(p-p')dp', \tag{5}$$

where A is a normalization coefficient.

The number of electrons emitted by the source material in the momentum interval Δp can be written in general form as

$$Q(p)=S(p)F(p)\psi(p),$$

where $S(p)$ is the phase space of β decay for electrons and $F(p)$ is the Fermi function which takes into account the Coulomb interaction of the β particle with the daughter nucleus. For our case

$$F(p)=2\pi x/[1-\exp(-2\pi x)], \quad x=2\alpha/\beta;$$

$\psi(p)$ represents all the other small corrections, including those due to uncertainty of the matrix element. As Bergkvist[11] has noted, the function $S(p)$ for the tritium of a real source differs substantially from the statistical shape (2) characterizing the decay of a free nucleus, as a result of the fact that on change of the charge of the nucleus the spectrum of stationary states of the electron shell also changes. In the general case with allowance both for the discrete spectrum of final states of the molecule and possible ionization (transition of a shell electron to the continuum) the function S has the form

$$S(p)=p^2\sum_i W_{1i}(E_0-E_i-E)[(E_0-E_i-E)^2-M_\nu^2]^{1/2}$$

$$+\int W_2(E')(E_0-E'-E)[(E_0-E'-E)^2-M_\nu^2]^{1/2}dE', \tag{6}$$

where W_{1i} and $W_2(E')$ are the probabilities of a transition to the discrete and continuous spectra and E_i and E' are the transition energies.

The exact spectrum of electronic states and transition probabilities can be calculated only for the atomic state of the source. In this case, neglecting the transition to the continuum (probability ~2.5%)[11] and, following Bergkvist, replacing the states 2S, 3S, and so forth by a single effective state with $E_2=43$ eV and $W_{12}=0.3$, we obtain a final formula for representation of the number of electrons measured in a channel

$$N(p_i)=A\sum_{k=i-I_{\max}}^{i-I_{\min}} F(p_k)p_k^3\{0.7(E_0-E_k)[(E_0-E_k)^2-M_\nu^2]^{1/2}$$

$$+0.3(E_0-43-E_k)[(E_0-43-E_k)^2-M_\nu^2]^{1/2}\}[1+\alpha(p_k-\tilde{p})]R(p_{i-k})+\Phi. \tag{7}$$

Here we have taken into account the assumed smallness of the energy dependence of the corrections, and the product $\psi(p)\varepsilon(p)\varphi(p)$ is represented in the form of the first term in a Taylor series in the vicinity of the point $\tilde{p}$—the middle of the measured energy interval; Φ is the spectrometer background, wnich does not depend on energy; $I_{\max}$ and $I_{\min}$ are the range of measurement of the instrumental function (for the proportional chamber $I_{\max}=15$ and $I_{\min}=-70$).

Equation (7) is a model (hypothesis) for the experimental data. It contains five parameters: $M_\nu, E_0, \alpha, A, \Phi$, two of which—$M_\nu$ and E_0, have physical meaning, i.e., they are related only to the β-decay process. The normalization and the background can be determined independently, but we knowingly include them in the number of adjustable parameters, thereby increasing the confidence interval for M_ν and E_0. For determination of the parameters of the model we seek the minimum of the functional

$$\chi^2(M_\nu, E_0, \alpha, A, \Phi)=\sum_{i=1}^{L}\left[\frac{N_e(p_i)-N(p_i)}{\sigma_i}\right]^2 \tag{8}$$

where $N_e(p_i)$ is the number of electrons recorded in channel I_i and σ_i is the dispersion of N_e. We have taken it equal to $(N_e)^{1/2}$.

In order to give the parameters M_ν and E_0 the physical meaning of the antineutrino mass and the β-transition energy, we have introduced natural limitations on the region of determination of χ^2 as functions of the parameters by the requirements

$$M_\nu^2\geqslant 0; \quad E_0\geqslant E; \quad (E_0-E)^2\geqslant M_\nu^2;$$
$$E_0-43\geqslant E; \quad (E_0-E-43)^2\geqslant M_\nu^2. \tag{9}$$

2. Results of search for optimal parameter values

First of all let us point out that no run intended for analysis was subsequently discarded. In each run we have recorded all channels. The results of the analysis of all 16 runs are given in the table.

In Fig. 8 we have shown as an example a portion of the experimental spectrum near the end point for run 11. For this run $\chi^2 = 128$ for a number of degrees of freedom $N_D = 107$. Small excesses of χ^2 over N_D of this type are observed in most of the runs. The experimental distribution of $\chi^2_N = \chi^2/N_D$ has a form corresponding to the expected distribution of $\chi^2_{N_D}$. However, this distribution is displaced: $\chi^2_N = 1.12 \pm 0.04$. The displacement is small and can be naturally explained by the fact that the statistical fluctuations of the counting rate do not determine the total error in Eq. (8). It is evident that an increase of all errors by 6% will already give an unshifted average value χ^2_N. However, although such an assumption is quite realistic, it is necessary first of all to be convinced that there is no lack of correspondence of the model (7) to the experimental spectrum within the limits of the difference of χ^2 and N_D. In all runs we checked the behavior of the value of χ^2 at each point along the energy axis and observed no systematic deviations which would indicate that the excess of the total χ^2 is collected as the result of a discrepancy between the model and experiment in any regions of energy. We shall show this in the example of the behavior of χ^2 on taking into account the sign of the discrepancy for three runs in Fig. 9 (runs 11, 12, and 13—the three channels of the proportional chamber in a single set of measurements). For these runs χ^2_N amounts to 1.21, 1.22, and 1.23 respectively and is somewhat greater than the average over the runs.

The choice of the variable ξ_k which characterizes the discrepancy in the form

$$\xi_k = \frac{(N_{ek} - N_k)^2}{N_{ek}} \operatorname{sign}(N_{ek} - N_k),$$

i.e., χ^2_k with the sign of the discrepancy for one point,

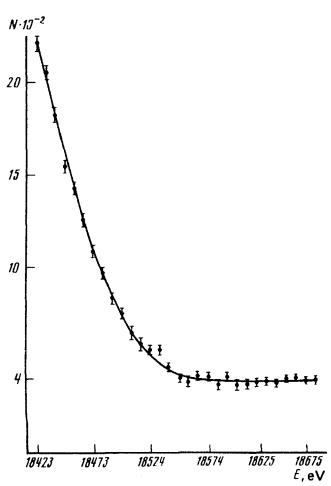

FIG. 8. High-energy part of the β spectrum (run 11). The solid curve is the optimum shape of the β spectrum (for the parameters see the table).

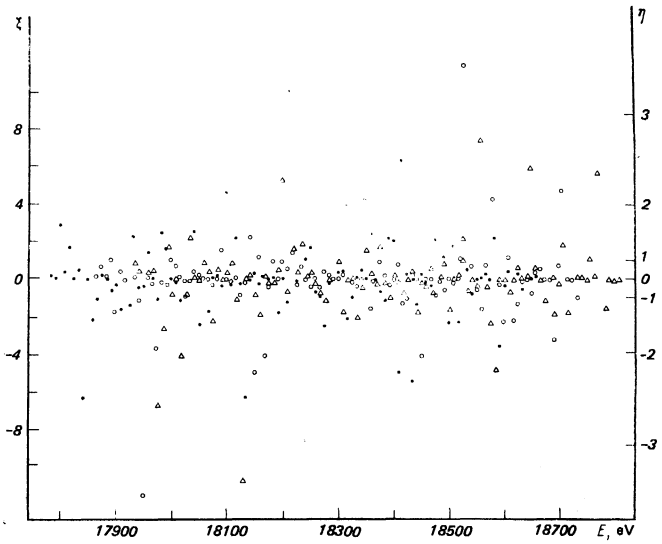

FIG. 9. Spread of experimental points with respect to the optimum β spectrum in the entire working region. ● —run 12, ○—run 11, △—run 13. The left-hand scale is χ^2 in the channel, ξ, and the right-hand scale is the relative discrepancy in the channel, η.

is convenient since for a correct model it corresponds to a distribution of χ^2 with one degree of freedom:

$$P(\xi) \sim \frac{\exp(-|\xi|/2)}{|\xi|^{1/2}} \frac{\xi}{|\xi|},$$

which diverges as $|\xi| \to 0$. This signifies a strong clustering of points at the place where the experiment agrees with the model. In Fig. 9 we can readily see that the clustering of points forms a straight line corresponding to $\xi = 0$. Thus, we do not observe a discrepancy between the model and experiment in any of the portions of the measured spectrum. From the same figure we can understand the cause of the discrepancy between χ^2 and N_D. At the right in Fig. 9 we have given the scale of deviations normalized to the statistical error, $\eta = (N_{ek} - N_k)/N_{ek}^{1/2}$. By projecting the points onto this scale we can determine how many events have a deviation exceeding one, two, and three standard deviations $N_{ek}^{1/2}$. It turns out that the distribution obtained corresponds, with an accuracy determined by the statistics, to a Gaussian distribution with zero mean and unit dispersion over the entire interval except for the discrepancies which exceed three standard deviations. In Fig. 9 there are five such discrepancies, compared to an expected number one. If we subtract the χ^2 of these points from the total χ^2 of all points:

$$\sum_{k=1}^{336} \chi_k^2 - \Sigma\chi^2(\xi > 10) = 389 - 59 = 330,$$

then the resulting value 330 ± 25 agrees with the number of degrees of freedom $331 - 15 = 316$. Similar discrepancies are encountered also in the remaining runs. In all 1636 points in the 16 runs there are 19 points with $\xi > 10$. All of the discrepancies are most likely random malfunctions in the detecting system. Analysis of all runs was carried out both without and with rejection of the points which gave $\xi > 10$. The values of the

parameters were practically unchanged by this. From this analysis ($\chi^2 \approx N_D$) we can draw two conclusions:

1) According to the χ^2 criterion, the model (7) of the β spectrum with the parameters given in the table agrees with the experimental data and the quantity (8) is distributed as χ^2.

2) The experimental data are characterized by a normal distribution with a dispersion $N^{1/2}$ (except for ~1% of the total number of points, the presence of which is not reflected in the parameter values).

Let us return to the table. In the eighth line we have given values of the parameter M_ν. These values do not depend on whether M_ν or M_ν^2 was used as an adjustable parameter. In the ninth line we have given values of the parameter E_0. Use for analysis in standard runs[12] and long runs of half of the energy range (a region which does not depend on the mass) gives no significant differences of E_0 from those given in the table. In the tenth and eleventh lines we have given values of the coefficient α and the correction $\alpha\Delta E$. In the lower parts of the seventh through eleventh lines we have given values obtained in a combined analysis of data obtained with the same type of detector. Note the value of the term $\alpha\Delta E$. The contribution of this term is ~12% for the proportional detector.[13] Use of this quantity in the form $\alpha(E-\bar{E})$ does not change this value or the values of the physical parameters. We carried out an optimization of the parameters with allowance for the next term in the expansion $\alpha(E-\bar{E})+\beta(E-\bar{E})^2$. It turned out that the second term amounts to 15% of the linear term with an error which exceeds this value. Inclusion of the quadratic term changes the value of χ^2 by ≈0.15% on the average over the runs, and the values of M_ν by an amount ≈1 eV, increasing M_ν. Thus, we consider that the use of a correction to the statistical shape of the β spectrum in linear form is justified under our conditions.

The optimum values of the background agree statistically with the values which can be calculated beforehand on the basis of the energy region above the β-spectrum end point with allowance for the resolution function. The parameter E_0 is distributed with a dispersion 5 eV about a mean value $E_0 = 18577 \pm 1.5$ eV.

In order to obtain the value of the β-decay energy, it is necessary to take into account the influence of chemical forces (internal potentials) on this quantity, and this must be done for all types of sources used in the work: the main sources, the layered sources, and the calibration sources. We did not carry out such an analysis. If, like Bergkvist, we set the uncertainty due to chemical effects equal to 10 eV, we obtain for the decay energy a value 18577 ± 12 eV. Thus, the discrepancy with Bergkvist's value[11] 18610 ± 16 eV, remains in effect. A histogram of the parameters M_ν is shown in Fig. 10. If we consider the 16 values of M_ν as a statistical sampling, then the average value is $\bar{M}_\nu = 35$ eV, the rms error in the phase space is $S_{M_\nu} = 13$ eV, and the rms error in $\bar{M}_\nu$ is 3.5 eV.

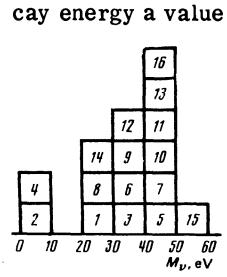

FIG. 10. Histogram of values of the parameter M_ν.

3. Confidence level for the antineutrino mass

The histogram shown in Fig. 10 gives the distribution of the most probable parameters M_ν corresponding to the conditions (9), but this is in no way the distribution of most probable values of the antineutrino mass. Note that the content of each channel of the histogram of M_ν is the sum over all the remaining parameters being optimized, i.e., it takes into account correlations between the parameters. To estimate the value of the antineutrino mass on the basis of the histogram it is necessary to know the density function of the distribution of the parameter M_ν for various hypotheses M_ν^* regarding the value of this mass. We shall designate it as $P(M_\nu|M_\nu^*)$. The characteristics of this function should depend on the experimental conditions: range of measured energies, intensity, background, resolution function, and so forth.

In the present work $P(M_\nu|M_\nu^*)$ was obtained by a Monte Carlo calculation according to the following scheme.

1. A spectrum N^s is generated for the range of energies, intensity, background, and the function R corresponding to the experimental conditions of the average standard run for fixed values of M_ν^* and the remaining parameters. For simulation of the statistics we used a sample from a normal distribution with a dispersion $(N^s)^{1/2}$.

2. A search is carried out for optimal parameters N^s with use of the model (7) and the conditions (9). By changing the sample of random numbers k times, we find k sets of $(M_\nu, E_0, \alpha, A, \Phi)$ which determine the function $P(M_\nu|M_\nu^*)$ summed over the remaining parameters, and the correlation function of M_ν with any of the parameters.

This procedure is good also in that, while the program for search for the minimum of the functional (8) has some previously unknown efficiency, this efficiency enters identically into the processing of the experimental data and the determination of $P(M_\nu|M_\nu^*)$. Consequently we have avoided program uncertainties. The same can be said of restrictions on the parameters—they have been taken into account in the function $P(M_\nu|M_\nu^*)$. In Fig. 11 we have shown several functions $P(M_\nu|M_\nu^*)$ for $M_\nu^* = 0$, 20, 40, and 50 eV. The conditions correspond to the standard run. For comparison we have shown by the dashed line the function $P(M_\nu|M_\nu^* = 0)$ for a spectrum with intensity increased by a factor of ten. We can see what the possibilities of the spectrometer are at different levels of statistics.

We can now answer the question: with what probability are the various mass hypotheses $P(M_\nu|M_\nu^*)$ compatible with the experimental histogram. We shall normalize all $P(M_\nu|M_\nu^*)$ to 16 events. Then in each chan-

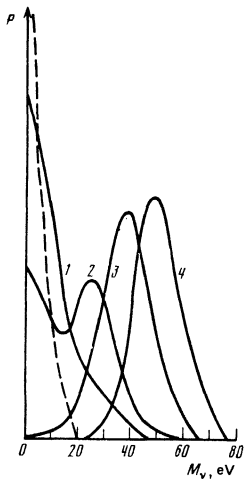

FIG. 11. Expectation function $P(M_\nu/M_\nu^*)$: 1—$P(M_\nu|0)$; 2—$P(M_\nu|20$ eV); 3—$P(M_\nu|40$ eV); 4—$P(M_\nu|50$ eV); the dashed curve is $P(M_\nu|0)$ for a tenfold increase of statistics.

nel of the histogram we can calculate the probability that we have a recorded number of events $N(M_\nu)$ if we expect $P(M_\nu|M_\nu^*)$ with a Poisson distribution. If we use the χ^2 test, the total value of this quantity on the basis of the entire histogram is shown in Fig. 12 (curve 1) for various M_ν^* hypotheses. The minimum of χ^2 occurs at the value $M_\nu^*=35$ eV and is equal to 7. For the 99% confidence interval we obtain from curve 1 the following estimate for the antineutrino mass value:

$$28\leqslant M_\nu^*\leqslant 41 \text{ eV}. \qquad (10)$$

We note that this estimate agrees with the direct estimate $\bar{M}_\nu=35$ eV based on the experimental histogram.

Up to this time the analysis of the parameters of the model has been carried out as a problem of mathematical statistics. In order to refine it let us consider the influence of variations of the resolution function R entering into (7). What changes in the mass estimate arise if we use in analysis of the experimental data a function R differing from the actual function? In order to evaluate the influence of variations of R, we can

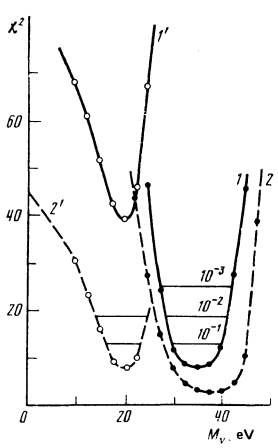

FIG. 12. Curves of compatibility of the distribution of the experimental parameters M_ν (Fig. 10) with $P(M_\nu|M_\nu^*)$: 1—two levels of $^3He^+$, 1′—one level of $^3He^+$, 2 and 2′—tne same for a cutoff M_ν histogram. The horizontal lines show the confidence levels.

process the experimental material with different R functions and trace the changes in the histogram of M_ν. On the other hand we can use a Monte Carlo procedure, evaluating the shifts in $P(M_\nu|M_\nu^*)$. The two methods, naturally, give identical results. We shall show them for the case of the functions $P(M_\nu|M_\nu^*)$.

Let us assume that we have made an error in our knowledge of R. Then let us use for generation of a quasi-experiment one (the "true") R^0, and in analysis of it another, R^{exp}: the one which was taken in calculation of the parameters from the experimental data. It turns out that if R^0 corresponds to a thinner source (i.e., if in the analysis we adopted a poorer resolution than the actual one), $P(M_\nu|M_\nu^*)$ will show a peak for values $M_\nu > M_\nu^*$. This is a dangerous situation. With a large difference of R^0 from R^{exp} even for $M_\nu^*=0$ a peak arises in the distribution in the parameter M_ν which simulates a nonexisting mass and can be taken as a manifestation of a mass of the antineutrino. The opposite situation in which R^0 is broader than R^{exp} we shall consider safe, since our estimate only reduces the true mass value.

Quantitative calculations showed that if instead of R^{exp} we had an R^0 corresponding to a source thickness a factor of two smaller than the actual one, we would erroneously increase the mass estimate by ~7 eV. In Fig. 13 we have shown the line shape from the standard source and from a source with half the thickness of valine. It can be seen from the figure that the difference in the lines is much greater than can be accepted on the basis of the method of their experimental determination.

An additional criterion of the accuracy of the function is the degree of agreement of the total resolution (the solid line in Fig. 9) and the line of a layered source covered with valine with a thickness half that of the working source thickness. The stability of the tritiated source is confirmed by data of measurements over many days. In Fig. 14 we have shown measurements of the M_I line of the calibration layered source during the time of recording runs 11 and 14. Here we have combined averaged data for 7 days (circles) and 12 days (dots).

In describing the procedure of the experimental determination it was pointed out that the wings of the instrumental line are determined with the greatest systematic error. We made a critical check of the influence of this uncertainty on the parameter M_ν in the

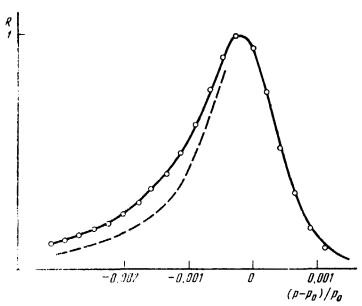

FIG. 13. Resolution function for a source with thickness 0.5 of the working thickness.

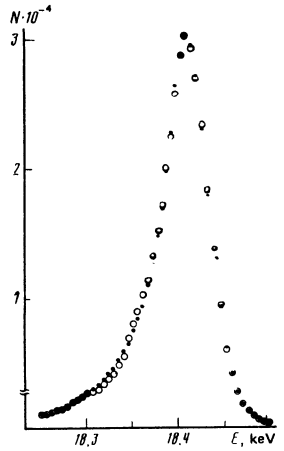

FIG. 14. Comparison of combined calibration peaks: o—sum of 7 measurements from April 21 to April 28, 1978; ●—sum of 12 measurements from May 10 to May 21, 1978. The background has been subtracted.

following way: the function R^{exp} was cut off on the low-energy side at a level 6% of the maximum value (20 channels for 160 eV). A new analysis of runs 11–16 showed the following set of parameters, with an insignificant change of χ^2:

Run	11	12	13	14	15	16
M_ν, eV	40.8	26.9	44.5	23.3	54.5	42.8

Here the parameter E_0 was practically unchanged. The behavior of the parameter α is interesting. Its value decreased by an amount $\sim 7 \cdot 10^{-4}$ eV^{-1}. This compensating ability of the parameter α is noted also in other modifications of the model (7), for example, on taking the linear factor out from under the integral sign in Eq. (5) or in changing the power p^3 to p^2, which corresponds to constancy of the momentum interval per channel. In all cases the physical parameters do not change significantly with appreciable changes of the parameter α. This indicates a linear influence on the spectrum of small changes in the model.[14)]

Summing up, we can say that if the β-decay spectrum of tritium in the source material corresponds to the atomic state of tritium [Eq. (6)] the estimate of the neutrino mass corresponds to the inequality (10). However, we cannot prove the statement that the tritium is in the atomic state and therefore the conclusion obtained cannot be regarded as adequately justified.

4. Lower limit for the masses

While adequate experimental justification existed for the restriction of the variations of the function R, we cannot calculate the wave functions of a molecule of the source in the T-He transition. Nevertheless this does not mean that we cannot pose the problem of the minimum value of antineutrino mass following from the experimental data under conditions of complete uncertainty as to the chemical nature of the source. Actually we know that an extended set of final states, like the instrumental line shape, further washes out the upper limit of the β spectrum.

Thus, if we introduce into the model of N_e the narrowest of all possible spectra of the final states of the molecule, namely a transition to one definite state (for example, the ground state), we obtain the maximum shift of the parameter M_ν. For determination of the numerical value of this shift we shall again use the method of the functions $P(M_\nu|M_\nu^*)$. In Fig. 15 we have shown the distribution of the parameter M_ν which arises for a true mass $M_\nu^*=0$ (curve 1) and $M_\nu^*=20$ eV (curve 2) if the transition to a single final state ($W_{11}=1, W_{12}=0$) is replaced by the atomic spectrum in the calculations. In Fig. 15 we have also shown the experimental histogram. It is evident that even for the maximum effect the hypothesis $M_\nu^*=0$ is incompatible with experiment.

To make an interval estimate with the minimum lower limit we again calculated the functions $P(M_\nu|M_\nu^*)$ for the set of M_ν^* and obtained a new compatibility curve (curve 1′ in Fig. 12). Note that the minimum of the compatibility curve has been raised to χ^2 values which are considerably above the acceptable values. This means that the experimental histogram is broader than the functions $P(M_\nu|M_\nu^*)$ for the spectrum with one final state. However, since we wish to obtain a model-free estimate, we shall take the hypothesis of a single state. Then the 99% confidence interval lies in the range

$$15 \leqslant M_\nu^* \leqslant 24 \text{ eV}. \tag{11}$$

Finally let us take a last step in a crude estimate of the mass. The calculated functions $P(M_\nu|M_\nu^*)$ may be inadequate for a real experiment. This will have its greatest effect in the tails, i.e., where the probabilities are low. We therefore carried out an analysis on the basis of compatibility curves with exclusion from consideration of the extreme channels of the experimental histogram (runs 2, 4, and 15). The loss of part of the information leads to a broadening of the compatibility curves (curves 2 and 2′ in Fig. 12) and consequently to an increase of the confidence interval:

$$14 \leqslant M_\nu^* \leqslant 26 \tag{12}$$

for the spectrum with one final state and

$$24 \leqslant M_\nu^* \leqslant 46 \tag{13}$$

for the spectrum of atomic tritium.

This important result compels us to point out the extreme assumptions which could make the lower mass

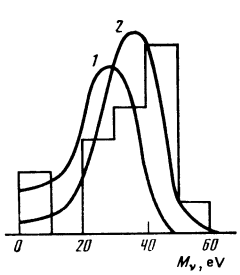

FIG. 15. The expectation function $P(M_\nu|M_\nu^*)$, corresponding to the maximum error in taking into account the $^3He^+$ final state; 1—$P(M_\nu|0)$; 2—$P(M_\nu|20$ eV). Also shown is the histogram of M_ν.

limit equal to zero. These assumptions will follow not from the experimental formulation itself nor from analysis of the properties of the apparatus, but from the desire to indicate the scale of errors which might be invented which will lead to substantial shifts of the mass. Since the influence of molecular effects has been taken into account to the maximum possible extent in the estimate (12), we shall discuss:

1) Large systematic uncertainties in the function R due to the fact that it is determined in additional experiments with layered sources.

2) Uncertainties in the correction function $1+\alpha(p-\tilde{p})$.

Let us imagine the unlikely situation in which, after the evaporation onto the substrate, the tritium of the working material, instead of being uniformly distributed over the thickness of the stopping layer, is located entirely on the surface facing the detector. Then the energy losses will affect the function R measured by transmission of a monochromatic line through the layer, but will not affect the line from the working source. In this case in the analysis we should take as R the instrumental line of pure ytterbium. Here the parameter M_ν would be decreased by 15 eV. Taking into account the uncertainty in the spectrum of final states, we would obtain an estimate of the lower limit close to zero. We note at once that if for some reason the tritium comes to the surface, it will most likely be in the atomic state. Then the estimate (13) is valid and again we cannot reconcile the experimental data with the hypothesis $M_\nu^*=0$.

There may be some broadening of the line in the layered source as a result of the fact that after covering the substrate with ytterbium, in the procedure for preparation of the layered sources, the vacuum is destroyed and between the ytterbium and the valine there may be a layer of air. However, in order to appreciably influence the mass estimate this layer should have a weight of half or more of the weight of the valine. The latter is inconsistent with the observed linear dependence of the losses on the thickness of the valine in the layered source.

An extremely subtle cause of inadequacy of our establishment of the function R by the method of layered sources has been suggested by Zel'dovich. If we imagine that the thickness of the valine layer is variable over the area of the source, then the instrumental line in the case of the layered source is formed by averaging with a weight proportional to the area covered by ytterbium, and in the case of the working source it is formed by averaging with a weight proportional to the volume of valine per unit area. However it can be shown that in this case the function R from the layered source will have a smaller width than the line of the working source, and such a substitution will only increase the lower mass limit.

The intrinsic width of the M lines can influence the correct determination of the function R. In our work it was assumed that this width is much less than the optical resolution of the spectrometer in the 18-keV region and does not affect the shape of its lines.

The correction $1+\alpha\Delta p$ could substantially affect the parameter M_ν if it were determined on the basis of additional measurements to have a highly distorted value (differing from optimal by a factor of two or three). We emphasize again that the value of α in our analysis was obtained in the processing together with the other parameters, and it was shown by modeling that the error in determination of this parameter does not exceed 15% and is taken into account in the histogram of M_ν.

IV. CONCLUSIONS

As we have said above, the existing experimental results do not give a sufficient basis for changing the estimates (12) and (13). Thus, independently of the influence of the chemical nature of the source material we arrive at the following conclusions.

1. The hypothesis $M_\nu^*=0$ is incompatible with the experimental data. We consider this an indication that at least one type of neutrino has nonzero mass.

2. The mass value lies in the 99% confidence interval which combines (12) and (13):

$$14\leqslant M_\nu^*\leqslant 46 \text{ eV}. \tag{14}$$

If, $M_\nu\neq 0$, then M_{ν_e}, M_{ν_μ}, and so forth are not mass eigenstates. Transitions (oscillations) are possible between neutrinos of different types.[18] In this case the statistical factor from Eq. (2) is an average over the mass eigenstates with weights determined by the mixing angles[19]:

$$S=\sum_i a_i(E_0-E)\left[(E_0-E)^2-M_{\nu_i}^2\right]^{1/2}.$$

However, the experimental accuracy is insufficient to identify a definite set of masses and mixing angles. Then the estimate (14) refers to a combination of the masses $M_{\nu_1}, M_{\nu_2}\ldots$ of the eigenstates:

$$M_\nu\approx(a_1M_{\nu_1}^2+a_2M_{\nu_2}^2+\ldots)^{1/2},\quad \Sigma a_i=1. \tag{15}$$

This relation is consistent with the experimental data, as was confirmed by a fit.

On the other hand if there are no oscillations of $\tilde{\nu}_e$ into neutrinos of other types, then the estimate (14) refers to the mass of the electron antineutrino:

$$M_\nu^*=M_{\tilde{\nu}_e}.$$

The results obtained in our work have been discussed extensively and this has been reflected in the present article. We are indebted to a large number of physicists who took active part in the discussions.

We are grateful to A. Aleksandrov, K. E. Bergkvist, Y. Galaktionov, S. Gershteĭn, Ya. Zel'dovich, I. Kaplan, L. Okun', B. Pontecorvo, K. Ter-Martirosyan, I. Chuvilo, A. Shal'nikov, and V. Shevchenko for discussion, interest, and support.

We extend our thanks to our colleagues of the laboratory who took part in the measurements and processing of the data—A. Apalikov, V. Konyaev, V. Okulovich, and V. Soloshchenko.

[1)]Here and below we have in mind the electron internal conversion lines from the transition with $E_\gamma = 20.74$ keV accompanied by electron capture in Yb^{169}. The daughter nucleus is Tm.
[2)]In the present work it was increased, which raised the accuracy.
[3)]The technology of preparation of the layered sources is described below.
[4)]By focusing current we mean the maximum of the line.
[5)]V. V. Shamanov took part in analysis of the calibration measurements.
[6)]A layer includes not only the material containing the tritium, but also impurities which were deposited on the substrate along with it.
[7)]The spectrum was measured in channel 0 of the three-channel chamber.
[8)]The cause of the broadening is unknown. It is most likely that it is a superposition of the K line of some γ transition.
[9)]The intensities of the two main sources turned out to be almost equal.
[10)]Actually if $Q(p') = \delta(p' - p_0)$ is the monochromatic line from internal conversion electrons, then it is evident from Eq. (4) that its instrumental representation will be $N(p) \sim \Delta p R(p, p_0)$. The function R measured on conversion lines is a folding of the optical line of the spectrometer and the energy loss function of the source material.
[11)]From the further analysis it will be evident that this approximation is justified, since a narrowing of the spectrum of final states will lead to a reduction of the estimate of the neutrino mass.
[12)]A standard run is defined as measurements in 112 channels with approximately identical statistics (for example, runs 9–16).
[13)]Thus, the initial assumption that ε, ψ, and φ are weak functions of energy was confirmed.
[14)]We can suggest that the rather high α value in runs 9 and 10, where the measurements were made with a low discrimination threshold, is due to a systematic error in determination of R for this measurement channel.

[1]E. F. Tret'yakov, N. F. Myasoedov, A. M. Apalikov, V. F. Konyaev, V. A. Lyubimov, and E. G. Novikov, Izv. AN SSSR, ser. fiz. 40, 2026 (1976) [Bull. USSR Acad. Sci., Phys. Ser. 40, No. 10, C1 (1976)]; Neutrino-76, Proc. of the Intern. Conf., Aachen, p. 663.
[2]V. S. Kozik, V. A. Lyubimov, E. G. Novikov, V. Z. Nozik, and E. F. Tret'yakov, Yad. Fiz. 32, 301 (1980) [Sov. J. Nucl. Phys. 32, 154 (1980)]; V. A. Lubimov, E. G. Novikov, V. Z. Nozik, E. F. Tratyakov, and V. S. Kozik, Phys. Lett. 94B, 266 (1980).
[3]G. C. Hanna and B. Pontecorvo, Phys. Rev. 75, 983 (1949).
[4]L. M. Langer and R. J. D. Moffat, Phys. Rev. 88, 689 (1952).
[5]D. R. Hamilton, W. P. Alford, and L. Gross, Phys. Rev. 92, 1521 (1953).
[6]F. T. Porter, Phys. Rev. 115, 450 (1959).
[7]R. C. Salgo and H. H. Staub, Nucl. Phys. A138, 417 (1969).
[8]R. Daris and C. St. Pierre, Nucl. Phys. A138, 545 (1969).
[9]V. E. Lewis, Nucl. Phys. A151, 120 (1970).
[10]B. Rode and H. Daniel, Lett. Nuovo Cimento 5, 139 (1972).
[11]K. E. Bergkvist, Ark. Fys. 27, 383, 439 (1964); Phys. Scripta 4, 23 (1971); Nucl. Phys. B39, 317 (1972).
[12]J. J. Simpson, Neutrino-79, Proc. of Intern. Conf., Bergen, 1979, Vol. 2, p. 208.
[13]E. F. Tret'yakov, Izv. An SSSR, ser. Fiz. 39, 583 (1975) [Bull. USSR Acad. Sci, Phys. Ser. 39, No. 3, 102 (1975)].
[14]Beta and Gamma-Ray Spectroscopy, edited by Kai Siegbahn, North Holland, Amsterdam, 1955. Russ. transl., Moscow, 1959, p. 102.
[15]K. Siegbahn (ed.), ESCA Applied to Free Molecules, North Holland, Amsterdam, 1970. Russ. transl., Mir, Moscow, 1971.
[16]V. A. Soloshchenko, Preprint ITEF-114, 1980.
[17]V. A. Soloshchenko, Yad. Fiz. 33, 1224 (1981) [Sov. J. Nucl. Phys. 33, No. 5, (1981) (in press)].
[18]B. M. Pontecorvo, Zh. Eksp. Teor. Fiz. 33, 549 (1957); 34, 247 (1958); 53, 1717 (1967) [Sov. Phys. JETP 6, 429 (1958); Sov. Phys. JEPT 7, 172 (1958); 26, 984 (1968)]. V. N. Gribov, and B. M. Pontecorvo, Phys. Lett. 28B, 493 (1969). S. M. Bilenky and B. M. Pontecorvo, Phys. Lett. 61B, 248 (1976).
[19]I. Yu. Kobzarev, B. V. Martemyanov, L. B. Okun, and M. G. Schepkin, Preprint ITEP-90, 1980.

Translated by Clark S. Robinson